Supplemental Figures and Legends

Table of Contents

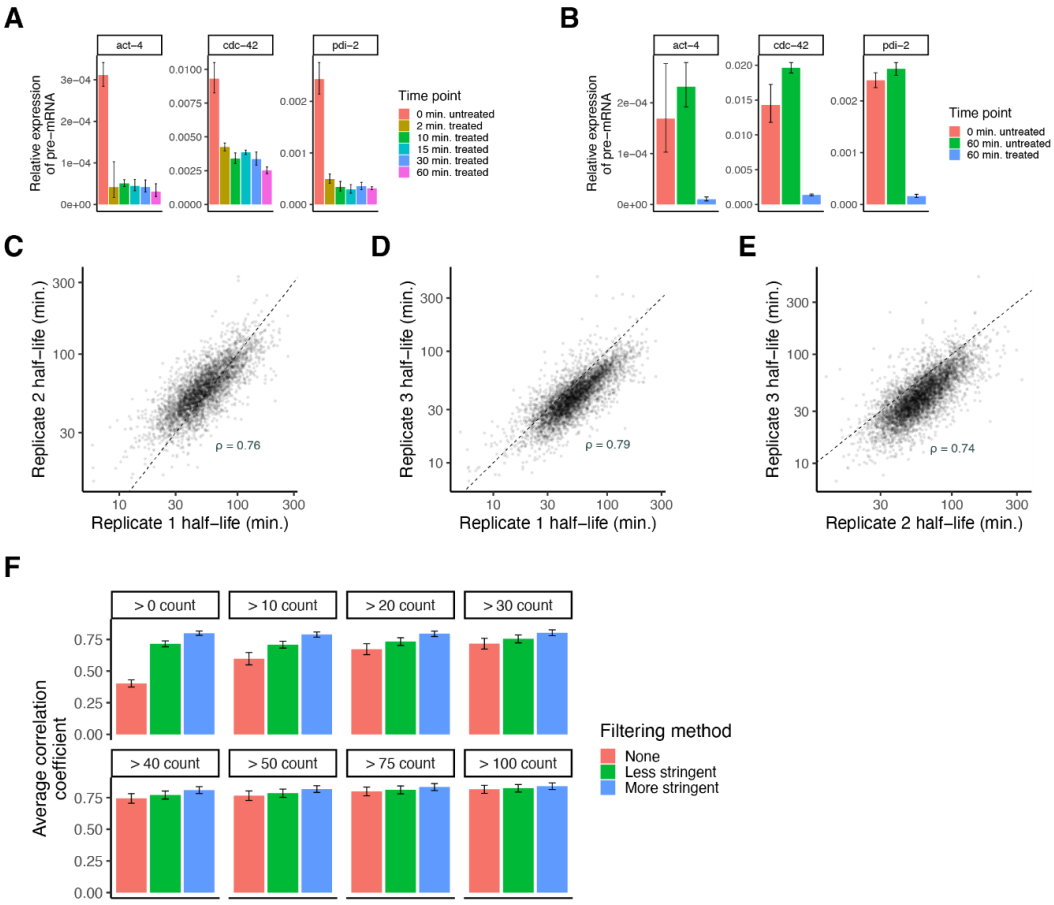
A
act−4
cdc−42
pdi−2
Relative expression of pre−mRNA
Time point
0 min. untreated
2 min. treated
10 min. treated
15 min. treated
30 min. treated
60 min. treated
B
act−4
cdc−42
pdi−2
Relative expression of pre−mRNA
Time point
0 min. untreated
60 min. untreated
60 min. treated
C
Replicate 2 half−life (min.)
Replicate 1 half−life (min.)
ρ = 0.76
D
Replicate 3 half−life (min.)
Replicate 1 half−life (min.)
ρ = 0.79
E
Replicate 3 half−life (min.)
Replicate 2 half−life (min.)
ρ = 0.74
F
> 0 count
> 10 count
> 20 count
> 30 count
> 40 count
> 50 count
> 75 count
> 100 count
Average correlation coefficient
Filtering method
None
Less stringent
More stringent

Supplemental Fig S1. Quality control for transcription inhibition approach paired with bulk RNA-sequencing. (A) Bar plots showing the relative expression of pre-mRNA for the housekeeping genes *act-4*, *cdc-42*, and *pdi-2* in embryonic cells following different lengths of transcription inhibition with actD. Expression was measured using RT-qPCR (quantitative reverse transcription PCR). Error bars represent variation in expression across three technical replicates. (B) Bar plots showing the relative expression of pre-mRNA for the housekeeping genes *act-4*, *cdc-42*, and *pdi-2* in embryonic cells following no treatment of actD, 60 minutes of treatment with actD, and 60 minutes with no treatment of actD. Expression was measured using RT-qPCR. Error bars represent variation in expression across three technical replicates. (C, D, E) Scatter plots showing the comparison of measured mRNA half-lives between three biological replicates on a log-log scale. Genes were compared if they had count > 30 at the 0 minute time point and if their decay fit an exponential decay model $R^2 \geq 0.75$ for each replicate. Spearman correlation coefficient is displayed for each pairwise comparison. Dashed line is the x = y line. (F) Bar plot showing the average Pearson correlation coefficient between mRNA half-lives across pairwise comparisons of three biological replicates under different count thresholds at the 0 minute time point and filtering methods. The less stringent filtering method only included genes if their coefficient of variation (standard deviation/mean*100) across biological replicates was ≤ 50% or the fold-change between the upper limit of their 95% confidence interval and measured half-life was ≤ 3. The stringent filtering method only included genes if their coefficient of variation across biological replicates was ≤ 30% or the fold-change between the upper limit of their 95% confidence interval and measured half-life was ≤ 2. Error bars represent standard deviation of the Pearson correlation coefficient among the three biological replicates.

A

Term	Expected	Observed	Enrichment.Fold.Change	P.value	Q.value
cytosolic large ribosomal subunit GO:0022625	3.8	25	6.5	0.0e+00	0.0e+00
extracellular region GO:0005576	21.0	62	2.9	7.2e−17	1.0e−14
structural constituent of ribosome GO:0003735	14.0	47	3.4	1.3e−16	1.2e−14
proton transmembrane transport GO:1902600	7.5	30	4.0	3.6e−14	2.5e−12
supramolecular polymer GO:0099081	37.0	79	2.1	6.6e−12	3.7e−10
calcium ion binding GO:0005509	15.0	41	2.8	3.0e−11	1.4e−09
muscle system process GO:0003012	7.2	26	3.6	4.1e−11	1.7e−09
structural constituent of chromatin GO:0030527	5.1	21	4.1	4.1e−11	1.7e−09
transmembrane transport GO:0055085	58.0	105	1.8	1.2e−10	3.6e−09
structural constituent of cytoskeleton GO:0005200	3.4	16	4.7	1.7e−10	4.9e−09
myofibril GO:0030016	13.0	37	2.8	1.8e−10	4.9e−09
actin binding GO:0003779	15.0	40	2.6	5.8e−10	1.4e−08
transporter activity GO:0005215	57.0	102	1.8	6.3e−10	1.4e−08
external encapsulating structure GO:0030312	7.1	24	3.4	1.1e−09	2.2e−08
purine nucleoside triphosphate metabolic process GO:0009144	4.5	17	3.8	1.4e−08	2.6e−07
protein heterodimerization activity GO:0046982	6.8	21	3.1	7.9e−08	1.4e−06
peptide biosynthetic process GO:0043043	39.0	71	1.8	1.5e−07	2.5e−06
muscle cell development GO:0055001	6.3	19	3.0	5.1e−07	8.1e−06
actin filament−based process GO:0030029	26.0	50	1.9	1.0e−06	1.5e−05
A band GO:0031672	5.2	16	3.1	2.4e−06	3.4e−05

B

Term	Expected	Observed	Enrichment.Fold.Change	P.value	Q.value
DNA−binding transcription factor activity GO:0003700	36.0	75	2.1	5.6e−11	1.6e−08
sequence−specific DNA binding GO:0043565	43.0	85	2.0	7.7e−11	1.6e−08
RNA biosynthetic process GO:0032774	85.0	140	1.6	6.4e−10	6.1e−08
cellular aromatic compound metabolic process GO:0006725	200.0	275	1.4	1.0e−09	7.1e−08
heterocycle metabolic process GO:0046483	200.0	274	1.4	1.4e−09	8.2e−08
organic cyclic compound metabolic process GO:1901360	200.0	275	1.4	3.5e−09	1.7e−07
transcription regulatory region nucleic acid binding GO:0001067	31.0	61	1.9	7.3e−08	3.0e−06
double−stranded DNA binding GO:0003690	36.0	67	1.9	8.9e−08	3.2e−06
condensed chromosome centromeric region GO:0000779	7.8	22	2.8	6.4e−07	2.0e−05
formation of primary germ layer GO:0001704	3.3	11	3.3	2.4e−05	6.8e−04
recombinational repair GO:0000725	5.1	14	2.8	5.3e−05	1.4e−03
metabolic process GO:0008152	410.0	475	1.2	1.2e−04	2.9e−03
protein−DNA complex GO:0032993	51.0	74	1.5	3.1e−04	6.8e−03
single−stranded DNA binding GO:0003697	3.8	10	2.6	7.2e−04	1.5e−02
nucleic acid transport GO:0050657	6.9	15	2.2	7.4e−04	1.5e−02
mRNA transport GO:0051028	5.1	12	2.4	8.5e−04	1.5e−02
meiotic cell cycle GO:0051321	20.0	33	1.7	1.1e−03	1.8e−02
RNA localization GO:0006403	7.1	15	2.1	1.2e−03	1.9e−02
cell−cell signaling by wnt GO:0198738	5.5	12	2.2	1.9e−03	2.9e−02
import into nucleus GO:0051170	5.2	11	2.1	3.7e−03	5.3e−02

C

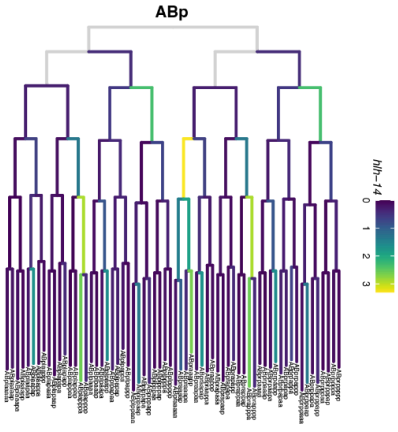

D

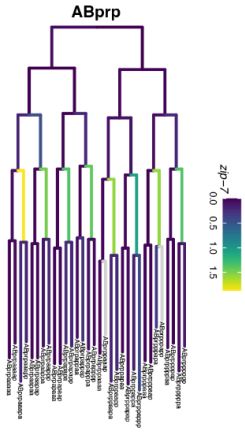

E

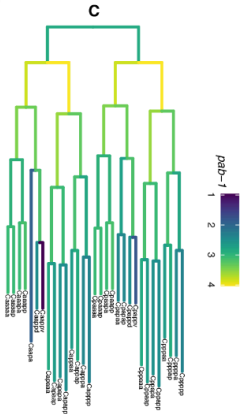

F

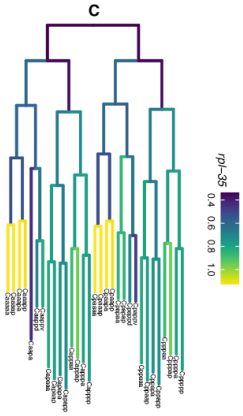

Supplemental Fig S2. Extended gene ontology analysis results for bulk data and lineage tree examples of highly transient and persistent genes. (A) Twenty most significantly enriched gene ontology terms for the top 15% stable transcripts. Background set of genes used was all genes that met our moderate mRNA half-life filtering metric. (B) Twenty most significantly enriched gene ontology terms for the top 15% unstable transcripts. Background set of genes used was all genes that met our moderate mRNA half-life filtering metric. (C, D, E, F) Sublineages with coloring representing gene expression from a *C. elegans* embryo single-cell mRNA atlas generated using single-cell RNA-sequencing (Packer et al. 2019).

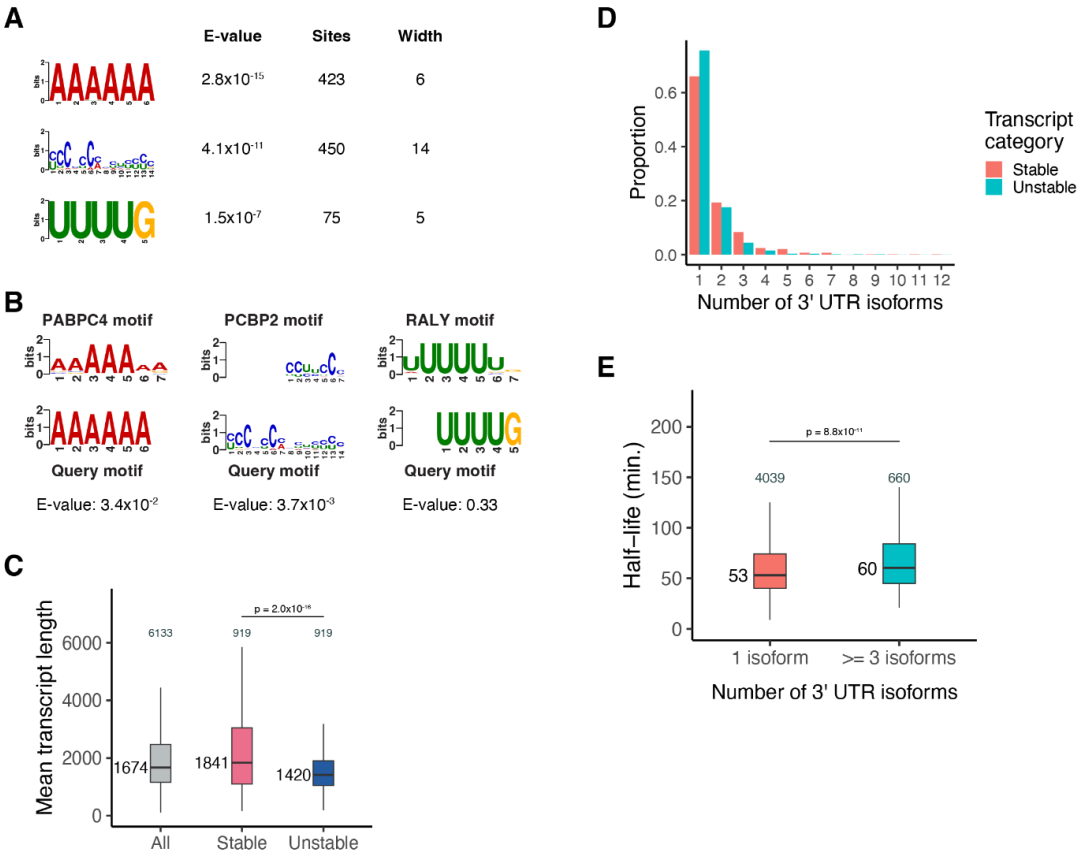
A
E-value
Sites
Width
2.8x10-15
423
6
4.1x10-11
450
14
1.5x10-7
75
5
B
PABPC4 motif
PCBP2 motif
RALY motif
Query motif
Query motif
Query motif
E-value: 3.4x10-2
E-value: 3.7x10-3
E-value: 0.33
C
Mean transcript length
p = 2.0x10-16
6133
919
919
1674
1841
1420
All
Stable
Unstable
D
Proportion
Number of 3' UTR isoforms
Transcript category
Stable
Unstable
E
Half−life (min.)
p = 8.8x10-11
4039
660
53
60
1 isoform
>= 3 isoforms
Number of 3' UTR isoforms

Supplemental Fig S3. Extended motif analysis results for stable transcripts in the bulk data and correlation between additional sequence attributes and mRNA stability. (A) Motifs found to be differentially enriched in the 3' UTRs of the top 15% stable transcripts using the *de novo* motif-finding program MEME (Bailey et al. 2015), including the E-value, number of sites found, and width for each motif. The 3' UTRs of the top 15% unstable transcripts were used as control sequences. (B) Mammalian motifs with the highest similarity to the motifs identified in (A) using the Tomtom motif comparison tool against a database of known motifs (Ray et al. 2013). (C) Distribution of transcript length averaged across all isoforms of a gene for the top 15% stable and unstable transcripts and all transcripts. Numbers to the left of the box plots are median values within each group. Numbers above the box plots are the number of genes within each group. P-value comparing median values was calculated using the Wilcoxon rank sum test. Outliers not shown. (D) Proportion of genes with the top 15% stable and unstable mRNA half-lives that have a certain number of 3' UTR isoforms. (E) Box plots showing the mRNA half-life distributions of genes having either one 3' UTR isoform or three or more 3' UTR isoforms. Numbers to the left of the box plots are median half-lives within each group. Numbers above the box plots are the number of genes within each group. P-value comparing median half-lives was calculated using the Wilcoxon rank sum test. Outliers not shown: from left to right, 111 and 23 genes within each group had mRNA half-lives > 150 minutes.

A

	E-value	Sites	Width
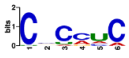	1.2x10^{-6}	173	6
	6.3x10^{-4}	137	5
	6.6x10^{-3}	173	12

B

PCBP2 motif	RBM46 motif	HuR motif
		
		
Query motif	Query motif	Query motif
E-value: 1.42	E-value: 2.75	E-value: 7.4x10^{-3}

C

	E-value	Sites	Width
	5.7x10^{-4}	78	11
	3.1x10^{-3}	74	10
	1.9x10^{-2}	65	7

D

HNRNPK motif	TIA1 motif	PCBP1 motif
		
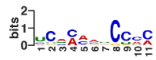		
Query motif	Query motif	Query motif
E-value: 9.4x10^{-2}	E-value: 8.5x10^{-4}	E-value: 6.9x10^{-2}

Supplemental Fig S4. Extended motif analysis results for genes that accumulate to high transcript levels. (A) Motifs found to be differentially enriched in the 3' UTRs of genes that accumulate to high transcript levels ~200 minutes past the four-cell stage in a whole embryo RNA-seq dataset (Hashimshony et al. 2015). Motifs were identified using the *de novo* motif-finding program MEME (Bailey et al. 2015). Table includes the E-value, number of sites found, and width for each motif. The 3' UTRs of genes that accumulate to low transcript levels ~200 minutes were used as control sequences. (B) Mammalian motifs with the highest similarity to the motifs identified in (A) using the Tomtom motif comparison tool against a database of known motifs (Ray et al. 2013). (C) Motifs found to be differentially enriched in the 3' UTRs of genes that accumulate to high transcript levels ~350 minutes past the four-cell stage in a whole embryo RNA-seq dataset (Hashimshony et al. 2015). Motifs were identified using the *de novo* motif-finding program MEME (Bailey et al. 2015). Table includes the E-value, number of sites found, and width for each motif. The 3' UTRs of genes that accumulate to low transcript levels ~350 minutes were used as control sequences. (D) Mammalian motifs with the highest similarity to the motifs identified in (C) using the Tomtom motif comparison tool against a database of known motifs (Ray et al. 2013).

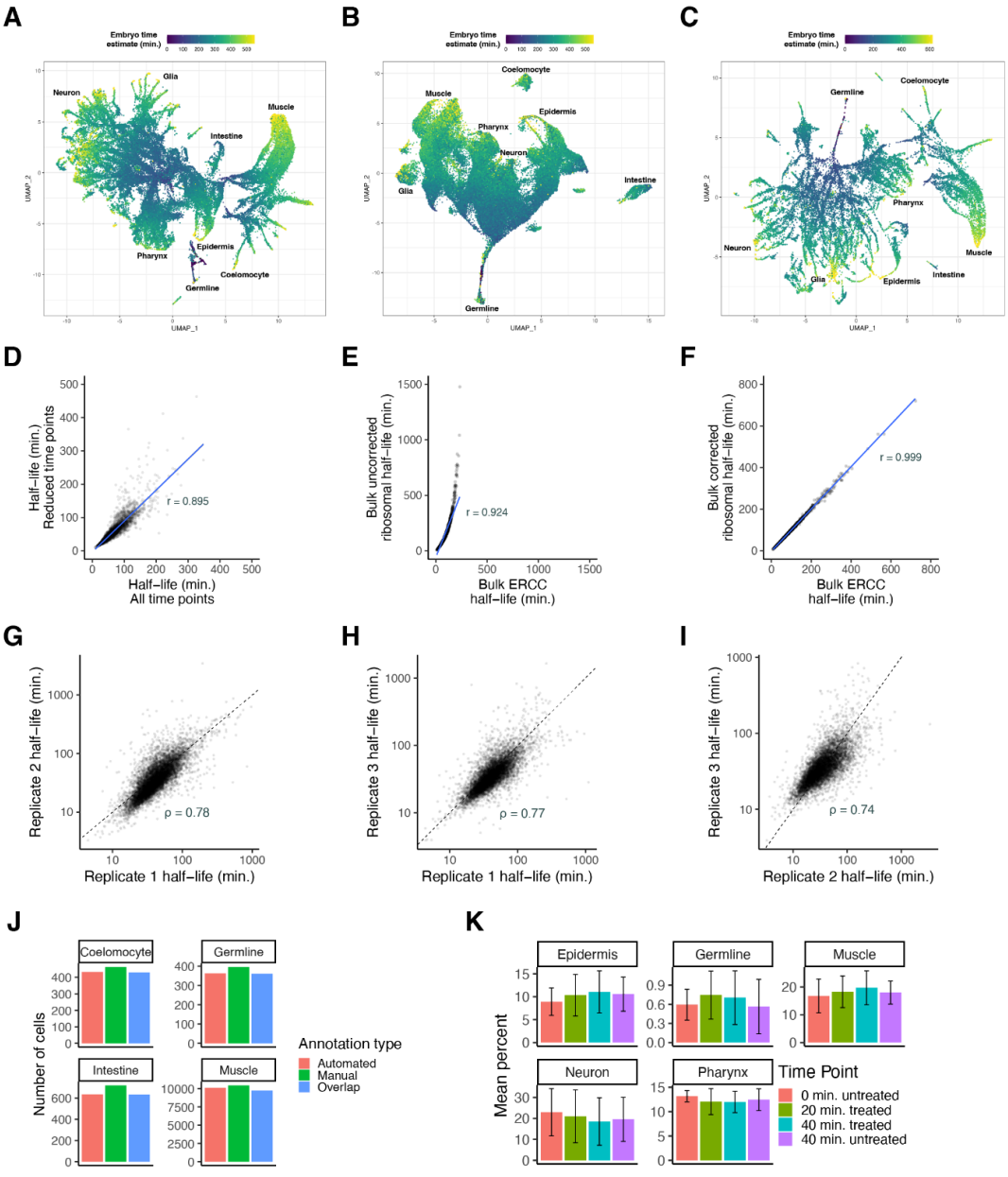
A
B
C
Embryo time estimate (min.)
Neuron
Glia
Muscle
Intestine
Pharynx
Epidermis
Coelomocyte
Germline
UMAP_1
UMAP_2
D
Half−life (min.) Reduced time points
Half−life (min.) All time points
r = 0.895
E
Bulk uncorrected ribosomal half−life (min.)
Bulk ERCC half−life (min.)
r = 0.924
F
Bulk corrected ribosomal half−life (min.)
Bulk ERCC half−life (min.)
r = 0.999
G
Replicate 2 half−life (min.)
Replicate 1 half−life (min.)
ρ = 0.78
H
Replicate 3 half−life (min.)
Replicate 1 half−life (min.)
ρ = 0.77
I
Replicate 3 half−life (min.)
Replicate 2 half−life (min.)
ρ = 0.74
J
Number of cells
Annotation type
Automated
Manual
Overlap
K
Mean percent
Time Point
0 min. untreated
20 min. treated
40 min. treated
40 min. untreated

Supplemental Fig S5. Quality control for transcription inhibition approach paired with single-cell RNA-sequencing. (A, B, C) Global UMAPs for individual biological replicates, with cells colored by embryo age as estimated from correlations to a whole-embryo RNA-sequencing time series (Hashimshony et al. 2015). Trajectories corresponding to major cell types are labeled. (D) Scatter plot showing the comparison of calculated mRNA half-lives when using all time points (0, 10, 20, 40, 60 minutes) or reduced time points (0, 20, 40 minutes) from the bulk data. Genes were compared if they met the following criteria: coefficient of variation across biological replicates ≤ 50% or the fold-change between the upper limit of their 95% confidence interval and measured half-life ≤ 3. To better include high-stability mRNAs, genes with half-lives > 100 minutes were allowed a looser filtering strategy. Such genes were included if their half-lives had a coefficient of variation ≤ 75% or fold-change between the upper limit of their 95% confidence interval and measured half-life ≤ 4. Pearson's correlation coefficient = 0.895. (E) Scatter plot showing the comparison in calculated mRNA half-lives from the bulk data between gene counts normalized to spike-in ERCC transcripts or transcripts encoding ribosomal proteins. Pearson's correlation coefficient = 0.924. Blue line is the best fit line. (F) Scatter plot showing the comparison in calculated mRNA half-lives from the bulk data between gene counts normalized to spike-in ERCC transcripts or transcripts encoding ribosomal proteins after correcting for their decay. Pearson's correlation coefficient = 0.999. Blue line is the best fit line. (G, H, I) Scatter plots showing the comparison of measured mRNA half-lives between 3 single-cell biological replicates on a log-log scale. Genes were compared if they had UMI > 30 at the 0 minute time point and if their decay fit an exponential decay model $R^2 \geq 0.75$ for each replicate. Spearman correlation coefficient is displayed for each pairwise comparison. Dashed line is the x = y line. (J) Bar plot comparing the number of cells from the first biological replicate annotated as coelomocyte, germline, intestine, or muscle based on manual annotation using marker genes or automated annotation using Seurat. (K) Bar plot showing the mean percentage of cells coming from the epidermis, germline, muscle, neuron, and pharynx within each biological replicate, separated by time point. Error bars represent standard deviation between the three biological replicates.

A

Group1	Group2	n1	n2	p	p.adjusted
Muscle	Germline	4350	802	2.21e−99	1.77e−98
Muscle	Epidermis	4350	3717	9.58e−06	1.92e−05
Muscle	Neuron	4350	4762	7.68e−30	3.84e−29
Muscle	Pharynx	4350	4700	7.00e−03	7.00e−03
Germline	Epidermis	802	3717	2.72e−75	1.90e−74
Germline	Neuron	802	4762	1.36e−186	1.36e−185
Germline	Pharynx	802	4700	1.78e−118	1.60e−117
Epidermis	Neuron	3717	4762	2.02e−55	1.21e−54
Epidermis	Pharynx	3717	4700	6.63e−13	1.99e−12
Neuron	Pharynx	4762	4700	1.00e−18	4.00e−18

B

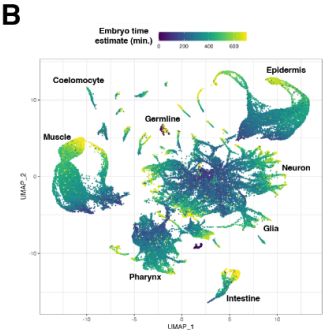

C

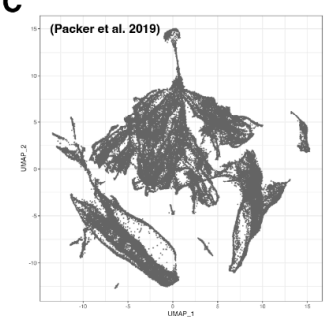

D

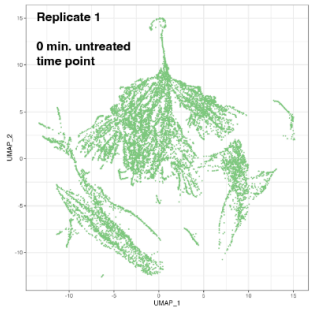

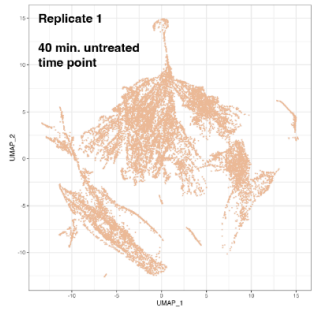

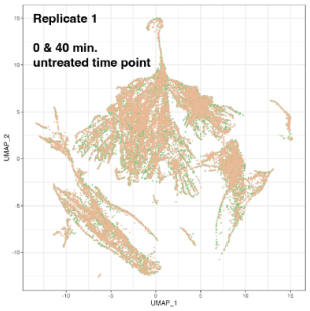

E

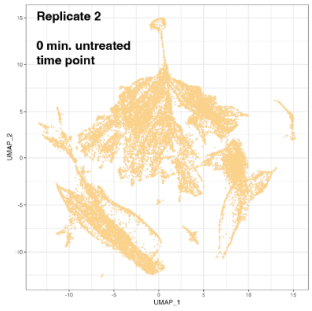

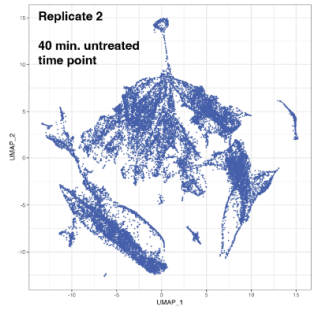

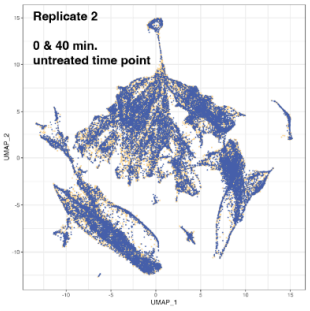

F

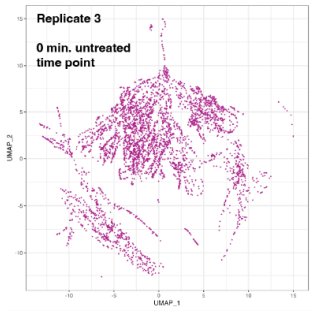

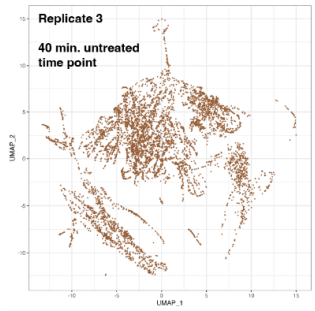

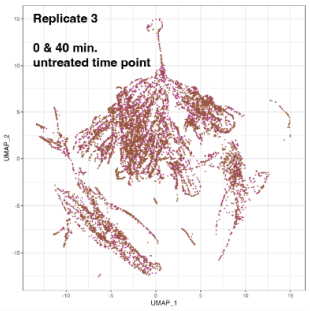

Supplemental Fig S6. Quality control for transcription inhibition approach paired with single-cell RNA-sequencing continued. (A) Table comparing the mRNA half-life distributions between epidermis, germline, muscle, neuron, and pharynx and whether the distributions are statistically significant from one another. P-values comparing median half-lives were calculated using the Wilcoxon rank sum test. (B) Global UMAP from a *C. elegans* embryo single-cell atlas (Packer et al. 2019). (C) UMAP projection of the integrated dataset of the three biological replicates with the existing *C. elegans* embryo single-cell atlas (Packer et al. 2019), colored by cells from (Packer et al. 2019). (D) UMAP projection of the integrated dataset of the three biological replicates with the existing *C. elegans* embryo single-cell atlas (Packer et al. 2019), colored by cells from the first biological replicate. (E) UMAP projection of the integrated dataset of the three biological replicates with the existing *C. elegans* embryo single-cell atlas (Packer et al. 2019), colored by cells from the second biological replicate. (F) UMAP projection of the integrated dataset of the three biological replicates with the existing *C. elegans* embryo single-cell atlas (Packer et al. 2019), colored by cells from the third biological replicate.

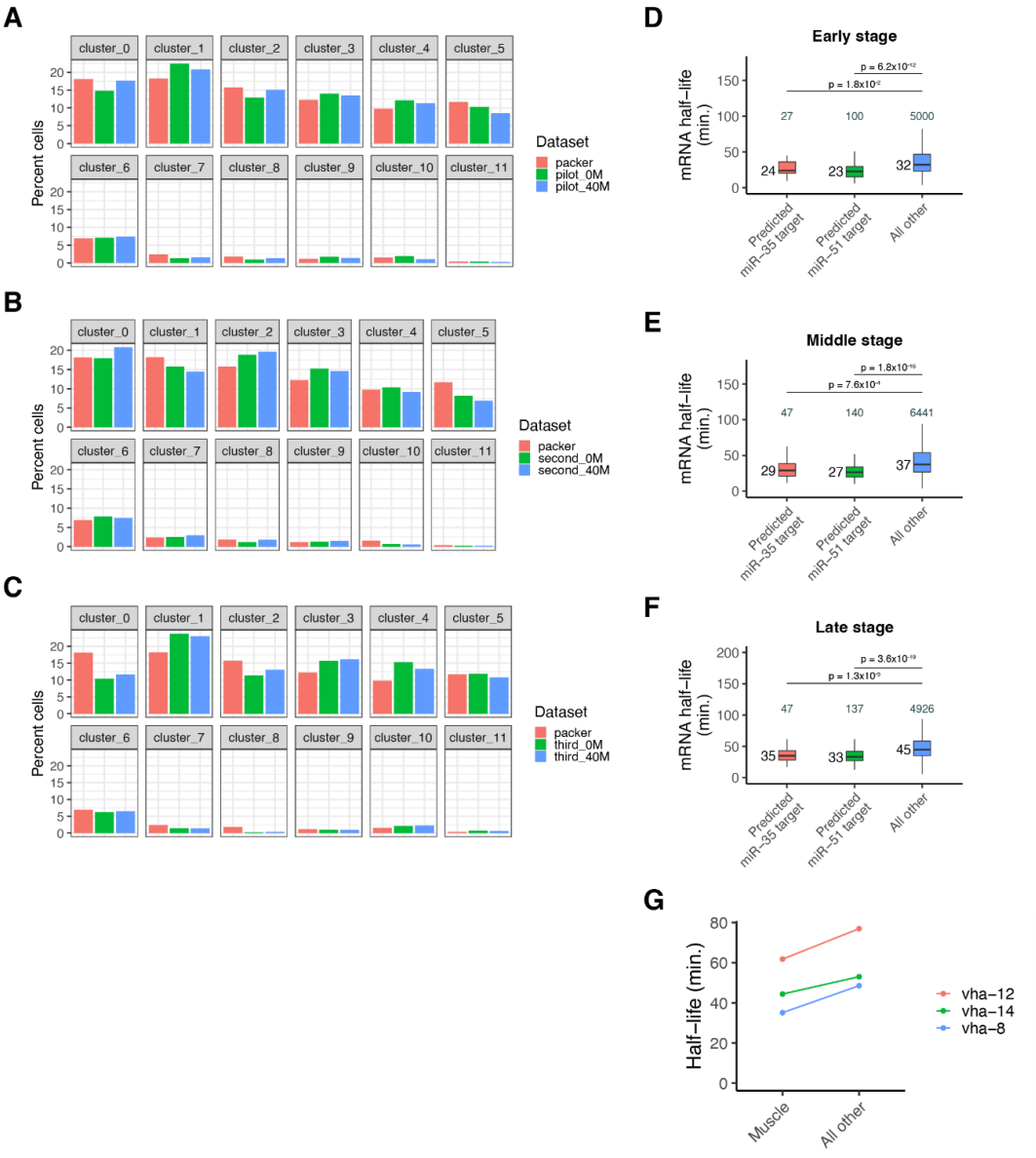
A
cluster_0
cluster_1
cluster_2
cluster_3
cluster_4
cluster_5
cluster_6
cluster_7
cluster_8
cluster_9
cluster_10
cluster_11
Percent cells
Dataset
packer
pilot_0M
pilot_40M
B
Dataset
packer
second_0M
second_40M
C
Dataset
packer
third_0M
third_40M
D
Early stage
p = 6.2x10⁻⁴²
p = 1.8x10⁻²
mRNA half-life (min.)
27
100
5000
24
23
32
Predicted miR-35 target
Predicted miR-51 target
All other
E
Middle stage
p = 1.8x10⁻¹⁵
p = 7.6x10⁻⁴
47
140
6441
29
27
37
F
Late stage
p = 3.6x10⁻¹⁹
p = 1.3x10⁻³
47
137
4926
35
33
45
G
Half-life (min.)
Muscle
All other
vha-12
vha-14
vha-8

Supplemental Fig S7. Quality control for transcription inhibition approach paired with single-cell RNA-sequencing continued and miRNA analysis. (A) Bar plot showing the percentage of cells from the (Packer et al. 2019) dataset, 0 minute untreated time point from the first biological replicate, and 40 minute untreated time point from the first biological replicate that correspond to clusters determined using the Louvain algorithm (Blondel et al. 2008). (B) Bar plot showing the percentage of cells from the (Packer et al. 2019) dataset, 0 minute untreated time point from the second biological replicate, and 40 minute untreated time point from the second biological replicate that correspond to clusters determined using the Louvain algorithm (Blondel et al. 2008). (C) Bar plot showing the percentage of cells from the (Packer et al. 2019) dataset, 0 minute untreated time point from the third biological replicate, and 40 minute untreated time point from the third biological replicate that correspond to clusters determined using the Louvain algorithm (Blondel et al. 2008). (D) Box plots showing the Early stage-specific mRNA half-life distributions of transcripts that are predicted targets of the miR-35 or miR-51 miRNA families or all other transcripts. Numbers to the left of the box plots are median half-lives within each group. Numbers above the box plots are the number of genes within each group. P-values comparing median half-lives were calculated using the Wilcoxon rank sum test. Outliers not shown: from left to right, 1, 2, and 200 genes within each group had mRNA half-lives > 100 minutes. (E) Box plots showing the Middle stage-specific mRNA half-life distributions of transcripts that are predicted targets of the miR-35 or miR-51 miRNA families or all other transcripts. Numbers to the left of the box plots are median half-lives within each group. Numbers above the box plots are the number of genes within each group. P-values comparing median half-lives were calculated using the Wilcoxon rank sum test. Outliers not shown: from left to right, 1, 3, and 341 genes within each group had mRNA half-lives > 100 minutes. (F) Box plots showing the Late stage-specific mRNA half-life distributions of transcripts that are predicted targets of the miR-35 or miR-51 miRNA families or all other transcripts. Numbers to the left of the box plots are median half-lives within each group. Numbers above the box plots are the number of genes within each group. P-values comparing median half-lives were calculated using the Wilcoxon rank sum test. Outliers not shown: from left to right, 2, 4, and 317 genes within each group had mRNA half-lives > 100 minutes. (G) Plot displaying mRNA half-lives specific to Middle and Late stage muscle cells or all other Middle and Late stage somatic cells for known miR-1 targets.

A

Term	Expected	Observed	Enrichment.Fold.Change	P.value	Q.value
structural constituent of chromatin GO:0030527	1.50	10	6.7	1.2e−07	3.5e−05
protein heterodimerization activity GO:0046982	2.20	10	4.6	6.9e−06	9.8e−04
transmembrane transport GO:0055085	9.10	20	2.2	3.3e−04	3.2e−02
passive transmembrane transporter activity GO:0022803	1.80	7	3.8	3.9e−04	3.2e−02
symporter activity GO:0015293	0.42	3	7.1	5.0e−04	3.2e−02
transporter activity GO:0005215	8.80	19	2.2	5.7e−04	3.2e−02

B

Term	Expected	Observed	Enrichment.Fold.Change	P.value	Q.value
cilium organization GO:0044782	2.400	19	8.1	2.5e−14	7.1e−12
non−motile cilium assembly GO:1905515	1.100	12	11.0	6.4e−12	9.1e−10
ciliary basal body GO:0036064	1.100	9	8.4	2.9e−08	2.7e−06
cell projection GO:0042995	12.000	31	2.6	5.0e−07	3.6e−05
cell projection organization GO:0030030	10.000	27	2.6	1.4e−06	8.0e−05
microtubule−based transport GO:0099111	1.800	9	5.0	8.0e−06	3.8e−04
non−motile cilium GO:0097730	1.200	7	6.0	1.2e−05	4.8e−04
ciliary plasm GO:0097014	0.690	5	7.3	2.9e−05	1.0e−03
taxis GO:0042330	5.500	15	2.7	1.3e−04	4.0e−03
supramolecular polymer GO:0099081	8.100	18	2.2	5.2e−04	1.5e−02
monoatomic ion homeostasis GO:0050801	2.400	8	3.3	5.5e−04	1.5e−02
inorganic ion import across plasma membrane GO:0099587	0.490	3	6.1	9.5e−04	2.2e−02
neurotransmitter receptor activity involved in regulation of postsynaptic membrane potential GO:0099529	0.098	1	10.0	2.4e−03	5.2e−02
transmembrane transport GO:0055085	10.000	19	1.9	3.4e−03	6.9e−02
synaptic signaling GO:0099536	3.700	9	2.4	3.9e−03	7.3e−02
sodium ion transport GO:0006814	0.730	3	4.1	5.1e−03	9.0e−02
passive transmembrane transporter activity GO:0022803	2.700	7	2.6	5.1e−03	9.0e−02
gated channel activity GO:0022836	1.200	4	3.4	5.5e−03	9.0e−02
monocarboxylic acid biosynthetic process GO:0072330	0.780	3	3.8	6.5e−03	9.7e−02
chemosensory behavior GO:0007635	1.200	4	3.3	6.5e−03	9.7e−02

C

Term	Expected	Observed	Enrichment.Fold.Change	P.value	Q.value
structural constituent of chromatin GO:0030527	0.59	4	6.8	0.00016	0.045
transmembrane transport GO:0055085	8.00	18	2.3	0.00039	0.055
peptidase inhibitor activity GO:0030414	0.43	3	7.0	0.00049	0.055
endopeptidase regulator activity GO:0061135	0.43	3	7.0	0.00049	0.055
extrinsic component of cytoplasmic side of plasma membrane GO:0031234	0.48	3	6.2	0.00085	0.055
extracellular region GO:0005576	1.60	6	3.7	0.00088	0.055
proteoglycan metabolic process GO:0006029	0.54	3	5.6	0.00140	0.055
inorganic ion import across plasma membrane GO:0099587	0.27	2	7.4	0.00140	0.055
protein serine kinase activity GO:0106310	3.40	9	2.6	0.00210	0.066
potassium ion transmembrane transport GO:0071805	0.32	2	6.2	0.00280	0.078
chloride channel complex GO:0034707	0.11	1	9.3	0.00290	0.078
monoatomic anion transport GO:0006820	0.65	3	4.6	0.00290	0.078
monoatomic ion homeostasis GO:0050801	2.00	6	2.9	0.00380	0.082
cytosolic large ribosomal subunit GO:0022625	0.70	3	4.3	0.00400	0.082
endoplasmic reticulum subcompartment GO:0098827	7.00	14	2.0	0.00430	0.082
transporter activity GO:0005215	7.70	15	1.9	0.00450	0.082
symporter activity GO:0015293	0.38	2	5.3	0.00460	0.082
sodium ion transport GO:0006814	0.38	2	5.3	0.00460	0.082
nuclear outer membrane−endoplasmic reticulum membrane network GO:0042175	7.30	14	1.9	0.00620	0.092

Supplemental Fig S8. Extended gene ontology analysis results for genes with more rapid mRNA decay over time. (A) Significantly enriched gene ontology terms for the top 5% of genes with faster decay in Middle-stage cells compared to Early-stage cells. Background set of genes used was shared genes between Early- and Middle-stage cells that met our moderate mRNA half-life filtering metric. (B) Twenty most significantly enriched gene ontology terms for the top 5% of genes with faster decay in Late-stage cells compared to Middle-stage cells. Background set of genes used was shared genes between Middle- and Late-stage cells that met our moderate mRNA half-life filtering metric. (C) Significantly enriched gene ontology terms for the top 5% of genes with faster decay in Late-stage cells compared to Early-stage cells. Background set of genes used was shared genes between Early- and Late-stage cells that met our moderate mRNA half-life filtering metric.

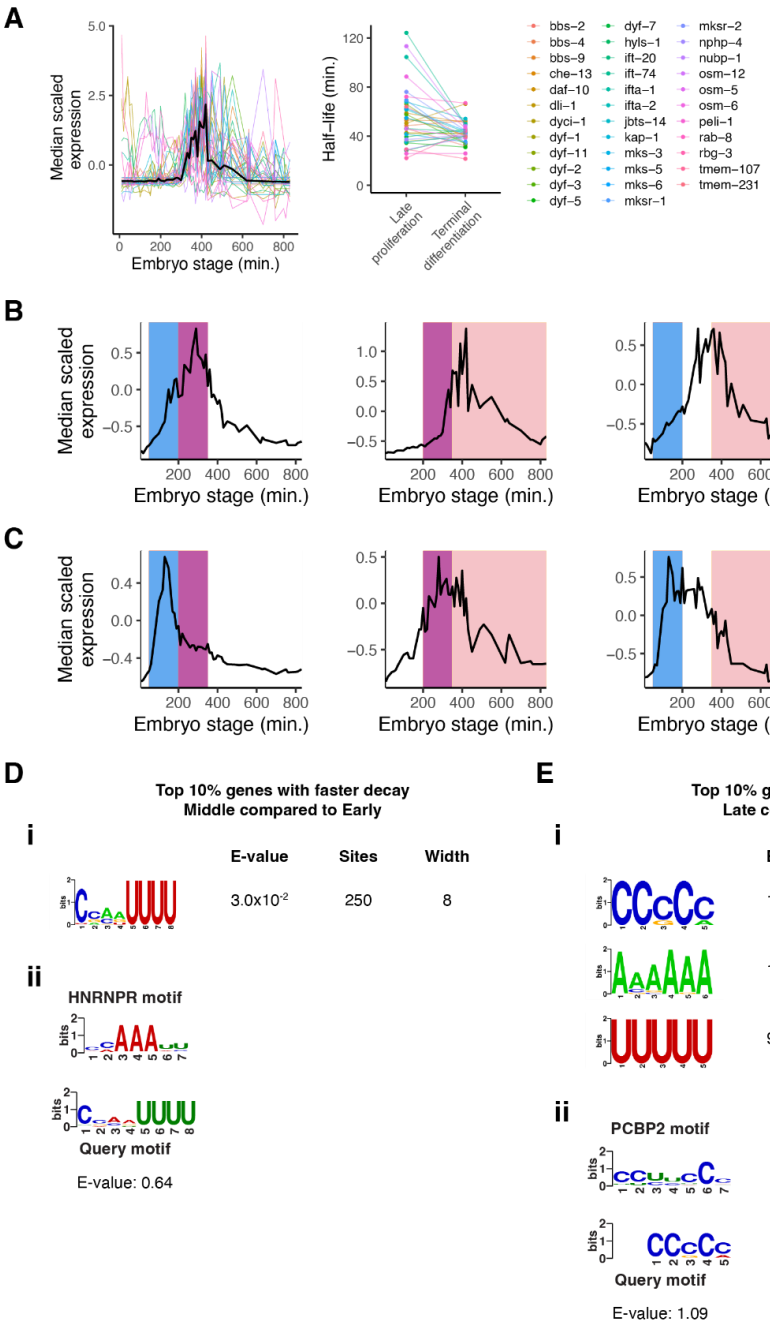
A
Median scaled expression
Embryo stage (min.)
Half-life (min.)
Late proliferation
Terminal differentiation
bbs−2
bbs−4
bbs−9
che−13
daf−10
dli−1
dyci−1
dyf−1
dyf−11
dyf−2
dyf−3
dyf−5
dyf−7
hyls−1
ift−20
ift−74
ifta−1
ifta−2
jbts−14
kap−1
mks−3
mks−5
mks−6
mksr−1
mksr−2
nphp−4
nubp−1
osm−12
osm−5
osm−6
peli−1
rab−8
rbg−3
tmem−107
tmem−231
B
C
D
Top 10% genes with faster decay
Middle compared to Early
i
E-value
Sites
Width
3.0x10-2
250
8
ii
HNRNPR motif
Query motif
E-value: 0.64
E
Top 10% genes with faster decay
Late compared to Middle
1.2x10-3
188
5
1.9x10-4
277
6
9.6x10-3
156
5
PCBP2 motif
PABPC4 motif
HNRNPC motif
E-value: 1.09
E-value: 3.9x10-3
E-value: 0.25

Supplemental Fig S9. Extended analyses for genes with differential mRNA decay over time. (A) *Left*. Median scaled expression of core cilia component genes using data from a whole-embryo RNA-sequencing time series (Hashimshony et al. 2015). *Right*. Plot displaying the change in mRNA half-lives from Middle to Late stage for core cilia component genes. (B) Median scaled expression of zygotic-only genes in the top 5% of genes with faster mRNA decay in a later stage compared to in an earlier stage. Blue shading spans the Early stage, purple shading spans the Middle stage, and pink shading spans the Late stage. (C) Median scaled expression of zygotic-only genes in the top 5% of genes with slower mRNA decay in a later stage compared to in an earlier stage. Blue shading spans the Early stage, purple shading spans the Middle stage, and pink shading spans the Late stage. (D) (i) Motif found to be differentially enriched in the 3' UTRs of the top 10% of genes with faster mRNA decay in the Middle stage compared to the Early stage. Motif was identified using the *de novo* motif-finding program MEME (Bailey et al. 2015). Table includes the E-value, number of sites found, and width for the motif. The 3' UTRs of the top 10% of genes with slower mRNA decay in the Middle stage compared to the Early stage were used as control sequences. (ii) Mammalian motif with the highest similarity to the motifs identified in (i) using the Tomtom motif comparison tool against a database of known motifs (Ray et al. 2013). (E) (i) Motifs found to be differentially enriched in the 3' UTRs of the top 10% of genes with faster mRNA decay in the Late stage compared to the Middle stage. Motifs were identified using the *de novo* motif-finding program MEME (Bailey et al. 2015). Table includes the E-value, number of sites found, and width for the motifs. The 3' UTRs of the top 10% of genes with slower mRNA decay in the Late stage compared to the Middle stage were used as control sequences. (ii) Mammalian motif with the highest similarity to the motifs identified in (i) using the Tomtom motif comparison tool against a database of known motifs (Ray et al. 2013).

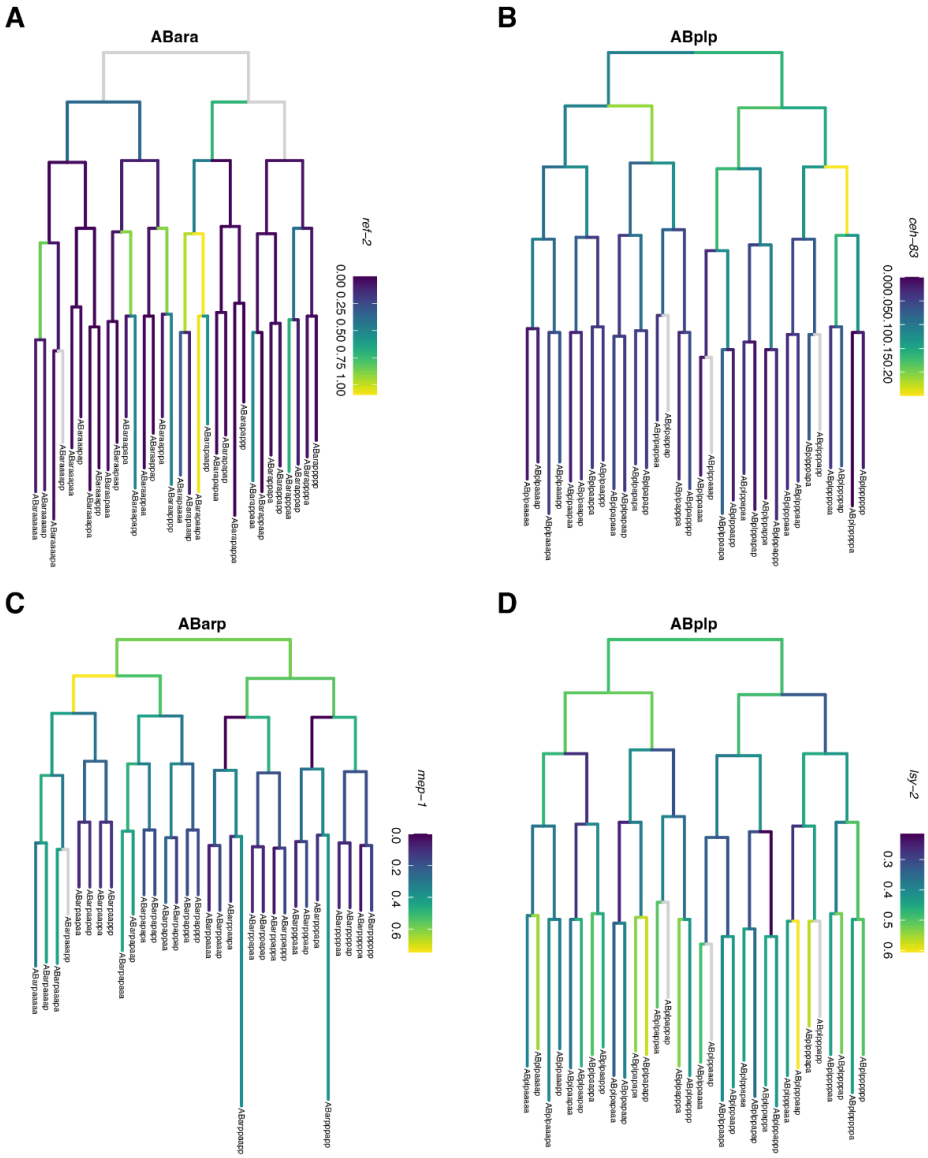
A
ABara
ref-2
0.00 0.25 0.50 0.75 1.00
B
ABplp
ceh-83
0.00 0.05 0.10 0.15 0.20
C
ABarp
mep-1
0.0 0.2 0.4 0.6
D
ABplp
lsy-2
0.3 0.4 0.5 0.6

Supplemental Fig S10. Lineage tree examples of transcription factor genes with transient or persistent mRNA expression. (A) Lineage tree for the ABara sublineage with coloring representing *ref-2* mRNA expression from our *C. elegans* embryo single cell atlas (Packer et al. 2019). (B) Lineage tree for the ABplp sublineage with coloring representing *ceh-83* mRNA expression from our *C. elegans* embryo single cell atlas (Packer et al. 2019). (C) Lineage tree for the ABarp sublineage with coloring representing *mep-1* mRNA expression from our *C. elegans* embryo single cell atlas (Packer et al. 2019). (D) Lineage tree for the ABplp sublineage with coloring representing *lsy-2* mRNA expression from our *C. elegans* embryo single cell atlas (Packer et al. 2019).

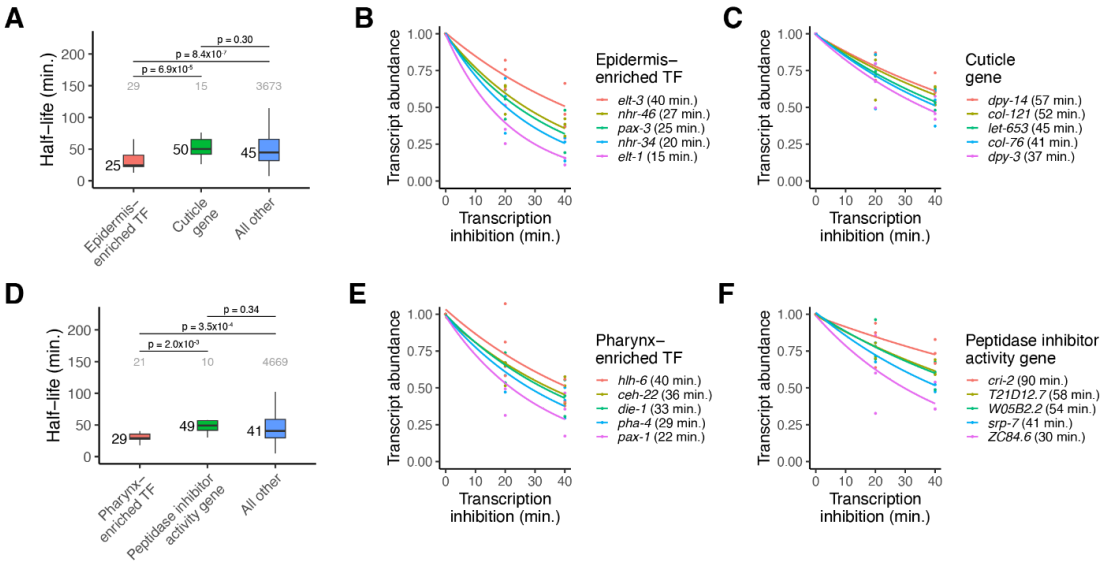
A
Half−life (min.)
p = 0.30
p = 8.4x10−7
p = 6.9x10−5
29
15
3673
25
50
45
Epidermis−enriched TF
Cuticle gene
All other
B
Transcript abundance
Transcription inhibition (min.)
Epidermis−enriched TF
elt-3 (40 min.)
nhr-46 (27 min.)
pax-3 (25 min.)
nhr-34 (20 min.)
elt-1 (15 min.)
C
Transcript abundance
Transcription inhibition (min.)
Cuticle gene
dpy-14 (57 min.)
col-121 (52 min.)
let-653 (45 min.)
col-76 (41 min.)
dpy-3 (37 min.)
D
Half−life (min.)
p = 0.34
p = 3.5x10−4
p = 2.0x10−3
21
10
4669
29
49
41
Pharynx−enriched TF
Peptidase inhibitor activity gene
All other
E
Transcript abundance
Transcription inhibition (min.)
Pharynx−enriched TF
hlh-6 (40 min.)
ceh-22 (36 min.)
die-1 (33 min.)
pha-4 (29 min.)
pax-1 (22 min.)
F
Transcript abundance
Transcription inhibition (min.)
Peptidase inhibitor activity gene
cri-2 (90 min.)
T21D12.7 (58 min.)
W05B2.2 (54 min.)
srp-7 (41 min.)
ZC84.6 (30 min.)

Supplemental Fig S11. mRNA half-lives of cell type-specific genes. (A) Box plots showing the epidermis-specific mRNA half-life distributions of epidermis-enriched transcription factor genes, cuticle genes, and all other genes. Numbers to the left of the box plots are median half-lives within each group. Numbers above box plots are the number of genes within each group. P-values comparing median half-lives were calculated using the Wilcoxon rank sum test. Outliers not shown: from left to right, 0, 0, and 150 genes within each group had mRNA half-lives > 150 minutes. (B) Scatter plot of the normalized transcript abundance of the epidermis-enriched transcription factor genes *elt-3*, *nhr-46*, *pax-3*, *nhr-34*, *elt-1* throughout a 40 minute transcription inhibition time course in epidermal cells. Each point represents normalized transcript abundance from one of three biological replicates. (C) Scatter plot of the normalized transcript abundance of the cuticle genes *dpy-14*, *col-121*, *let-653*, *col-76*, *dpy-3* throughout a 40 minute transcription inhibition time course in epidermal cells. Each point represents normalized transcript abundance from one of three biological replicates. (D) Box plots showing the pharynx-specific mRNA half-life distributions of pharynx-enriched transcription factor genes, peptidase inhibitor activity genes, and all other genes. Numbers to the left of the box plots are median half-lives within each group. Numbers above box plots are the number of genes within each group. P-values comparing median half-lives were calculated using the Wilcoxon rank sum test. Outliers not shown: from left to right, 0, 0, and 125 genes within each group had mRNA half-lives > 150 minutes. (E) Scatter plot of the normalized transcript abundance of the pharynx-enriched transcription factor genes *hlh-6*, *ceh-22*, *die-1*, *pha-4, pax-1* throughout a 40 minute transcription inhibition time course in pharynx cells. Each point represents normalized transcript abundance from one of three biological replicates. (F) Scatter plot of the normalized transcript abundance of the peptidase inhibitor activity genes *cri-2*, *T21D12.7*, *W05B2.2*, *srp-7*, *ZC84.6* throughout a 40 minute transcription inhibition time course in pharynx cells. Each point represents normalized transcript abundance from one of three biological replicates.

A

Term	Expected	Observed	Enrichment.Fold.Change	P.value	Q.value
supramolecular polymer GO:0099081	9.9	50	5.1	3.8e−23	5.4e−21
striated muscle dense body GO:0055120	4.5	33	7.4	3.7e−22	3.5e−20
myofibril GO:0030016	3.6	29	8.1	2.8e−21	2.0e−19
extracellular region GO:0005576	3.6	25	7.0	1.1e−16	6.4e−15
A band GO:0031672	1.7	17	10.0	6.0e−16	2.8e−14
muscle system process GO:0003012	1.7	17	9.9	1.5e−15	6.0e−14
sarcomere organization GO:0045214	1.5	16	10.0	2.6e−15	9.1e−14
gated channel activity GO:0022836	2.3	18	8.0	5.6e−14	1.8e−12
passive transmembrane transporter activity GO:0022803	4.2	24	5.7	1.4e−13	3.9e−12
muscle cell development GO:0055001	2.1	17	7.9	2.6e−13	6.7e−12

B

Term	Expected	Observed	Enrichment.Fold.Change	P.value	Q.value
cell projection organization GO:0030030	14.0	78	5.4	4.7e−36	3.4e−36
cilium organization GO:0044782	3.8	41	11.0	4.8e−38	3.4e−36
cell projection GO:0042995	18.0	86	4.8	9.8e−37	4.7e−35
ciliary basal body GO:0036064	2.0	25	13.0	1.3e−27	5.3e−26
non−motile cilium assembly GO:1905515	1.7	21	12.0	3.9e−23	1.4e−21
ciliary plasm GO:0097014	1.1	15	14.0	2.2e−19	6.8e−18
taxis GO:0042330	8.1	37	4.6	2.2e−16	6.1e−15
neuron development GO:0048666	8.8	37	4.2	5.8e−15	1.5e−13
microtubule−based transport GO:0099111	2.6	19	7.3	4.6e−14	1.1e−12
extracellular region GO:0005576	3.2	17	5.3	6.6e−10	1.4e−08

C

Term	Expected	Observed	Enrichment.Fold.Change	P.value	Q.value
extracellular region GO:0005576	3.70	24	6.6	1.5e−15	8.4e−14
molting cycle GO:0042303	2.50	19	7.7	1.9e−14	8.8e−13
organic acid metabolic process GO:0006082	9.40	37	3.9	6.0e−14	2.4e−12
structural constituent of cuticle GO:0042302	0.72	9	13.0	1.4e−11	5.0e−10
oxidoreductase activity acting on CH−OH group of donors GO:0016614	1.90	11	5.8	1.0e−07	3.3e−06
DNA−binding transcription factor activity GO:0003700	9.30	27	2.9	1.4e−07	4.1e−06
microbody GO:0042579	1.60	10	6.1	1.7e−07	4.3e−06
zinc ion binding GO:0008270	7.90	24	3.0	2.3e−07	5.3e−06
iron ion binding GO:0005506	1.20	8	6.5	1.1e−06	2.3e−05
peptidase inhibitor activity GO:0030414	0.59	5	8.5	5.4e−06	1.1e−04

D

Term	Expected	Observed	Enrichment.Fold.Change	P.value	Q.value
serine−type endopeptidase inhibitor activity GO:0004867	0.18	7	40.0	5.4e−14	7.7e−12
peptidase inhibitor activity GO:0030414	0.26	7	28.0	2.5e−11	2.4e−09
endopeptidase regulator activity GO:0061135	0.29	7	24.0	6.3e−11	4.5e−09
DNA−binding transcription factor activity GO:0003700	4.10	19	4.6	6.6e−09	3.8e−07
transcription regulatory region nucleic acid binding GO:0001067	3.80	17	4.5	5.7e−08	2.7e−06
sequence−specific DNA binding GO:0043565	5.20	19	3.7	3.1e−07	1.2e−05
double−stranded DNA binding GO:0003690	4.40	17	3.9	5.6e−07	2.0e−05
pharynx development GO:0060465	0.53	6	11.0	6.2e−07	2.0e−05
cell surface GO:0009986	0.46	5	11.0	4.6e−06	1.3e−04
external encapsulating structure GO:0030312	0.46	4	8.6	7.8e−05	2.0e−03

E

Term	Expected	Observed	Enrichment.Fold.Change	P.value	Q.value
mRNA 3'−UTR binding GO:0003730	4.3	8	1.8	0.0014	0.014
membrane−enclosed lumen GO:0031974	73.0	90	1.2	0.0019	0.018
single−stranded DNA binding GO:0003697	3.4	6	1.8	0.0051	0.056
recombinational repair GO:0000725	3.4	6	1.8	0.0051	0.056
cell part morphogenesis GO:0032990	3.4	6	1.8	0.0051	0.056
neuron development GO:0048666	2.9	5	1.7	0.0130	0.110
identical protein binding GO:0042802	9.7	14	1.4	0.0140	0.110
import into nucleus GO:0051170	5.3	8	1.5	0.0250	0.200
ATP−dependent activity acting on RNA GO:0008186	5.3	8	1.5	0.0250	0.200
extracellular region GO:0005576	2.4	4	1.7	0.0260	0.200

Supplemental Fig S12. Gene ontology analysis of cell type-specific genes. (A) Ten most significantly enriched gene ontology terms for muscle-specific genes that met our moderate mRNA half-life filtering metric within muscle cells. Background set of genes used was all genes that met our moderate mRNA half-life filtering metric within muscle cells. (B) Ten most significantly enriched gene ontology terms for neuron-specific genes that met our moderate mRNA half-life filtering metric within neuronal cells. Background set of genes used was all genes that met our moderate mRNA half-life filtering metric within neuron cells. (C) Ten most significantly enriched gene ontology terms for epidermis-specific genes that met our moderate mRNA half-life filtering metric within epidermal cells. Background set of genes used was all genes that met our moderate mRNA half-life filtering metric within epidermal cells. (D) Ten most significantly enriched gene ontology terms for pharynx-specific genes that met our moderate mRNA half-life filtering metric within pharynx cells. Background set of genes used was all genes that met our moderate mRNA half-life filtering metric within pharynx cells. (E) Ten most significantly enriched gene ontology terms for germline-specific genes that met our moderate mRNA half-life filtering metric within germline cells. Background set of genes used was all genes that met our moderate mRNA half-life filtering metric within germline cells.

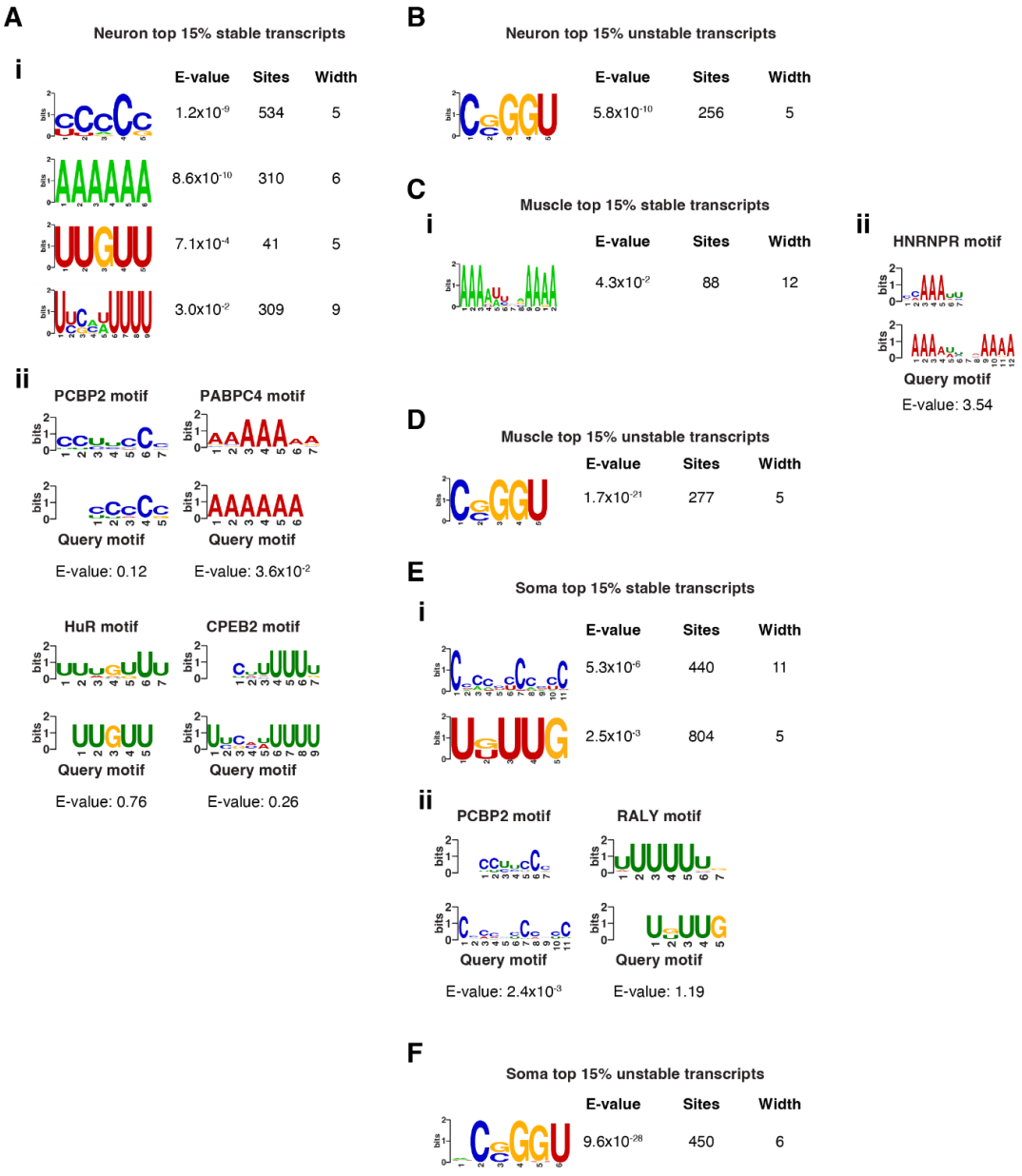
A
Neuron top 15% stable transcripts
i
E-value
Sites
Width
1.2x10-9
534
5
8.6x10-10
310
6
7.1x10-4
41
5
3.0x10-2
309
9
ii
PCBP2 motif
PABPC4 motif
Query motif
Query motif
E-value: 0.12
E-value: 3.6x10-2
HuR motif
CPEB2 motif
Query motif
Query motif
E-value: 0.76
E-value: 0.26
B
Neuron top 15% unstable transcripts
E-value
Sites
Width
5.8x10-10
256
5
C
Muscle top 15% stable transcripts
i
E-value
Sites
Width
4.3x10-2
88
12
ii
HNRNPR motif
Query motif
E-value: 3.54
D
Muscle top 15% unstable transcripts
E-value
Sites
Width
1.7x10-21
277
5
E
Soma top 15% stable transcripts
i
E-value
Sites
Width
5.3x10-6
440
11
2.5x10-3
804
5
ii
PCBP2 motif
RALY motif
Query motif
Query motif
E-value: 2.4x10-3
E-value: 1.19
F
Soma top 15% unstable transcripts
E-value
Sites
Width
9.6x10-28
450
6

Supplemental Fig S13. Motif analysis for stable and unstable transcripts within somatic cell types. (A) (i) Motifs found to be differentially enriched in the 3' UTRs of the top 15% stable genes within neurons. Motifs were identified using the *de novo* motif-finding program MEME (Bailey et al. 2015). Table includes the E-value, number of sites found, and width for the motifs. The 3' UTRs of the top 15% unstable genes within neurons were used as control sequences. (ii) Mammalian motifs with the highest similarity to the motifs identified in (i) using the Tomtom motif comparison tool against a database of known motifs (Ray et al. 2013). (B) Motif found to be differentially enriched in the 3' UTRs of the top 15% unstable genes within neurons. Motif was identified using the *de novo* motif-finding program MEME (Bailey et al. 2015). Table includes the E-value, number of sites found, and width for the motif. The 3' UTRs of the top 15% stable genes within neurons were used as control sequences. C) (i) Motif found to be differentially enriched in the 3' UTRs of the top 15% stable genes within muscle. Motif was identified using the *de novo* motif-finding program MEME (Bailey et al. 2015). Table includes the E-value, number of sites found, and width for the motif. The 3' UTRs of the top 15% unstable genes within muscle were used as control sequences. (ii) Mammalian motif with the highest similarity to the motifs identified in (i) using the Tomtom motif comparison tool against a database of known motifs (Ray et al. 2013). (D) Motif found to be differentially enriched in the 3' UTRs of the top 15% unstable genes within muscle. Motif was identified using the *de novo* motif-finding program MEME (Bailey et al. 2015). Table includes the E-value, number of sites found, and width for the motif. The 3' UTRs of the top 15% stable genes within muscle were used as control sequences. (E) (i) Motifs found to be differentially enriched in the 3' UTRs of the top 15% stable genes within the soma. Motifs were identified using the *de novo* motif-finding program MEME (Bailey et al. 2015). Table includes the E-value, number of sites found, and width for the motifs. The 3' UTRs of the top 15% unstable genes within the soma were used as control sequences. (ii) Mammalian motifs with the highest similarity to the motifs identified in (i) using the Tomtom motif comparison tool against a database of known motifs (Ray et al. 2013). (F) Motif found to be differentially enriched in the 3' UTRs of the top 15% unstable genes within the soma. Motif was identified using the *de novo* motif-finding program MEME (Bailey et al. 2015). Table includes the E-value, number of sites found, and width for the motif. The 3' UTRs of the top 15% stable genes within the soma were used as control sequences.

A

Term	Expected	Observed	Enrichment.Fold.Change	P.value	Q.value
detoxification GO:0098754	0.07	1	14.0	0.00000	0.000
cellular oxidant detoxification GO:0098869	0.07	1	14.0	0.00000	0.000
guanyl−nucleotide exchange factor activity GO:0005085	0.21	2	9.5	0.00035	0.033
post−transcriptional gene silencing GO:0016441	0.49	3	6.1	0.00071	0.051
peptide biosynthetic process GO:0043043	4.60	11	2.4	0.00170	0.095

B

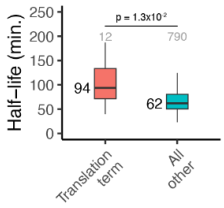

C

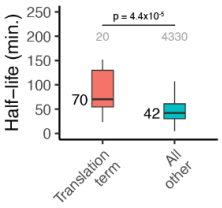

D

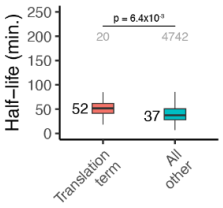

E

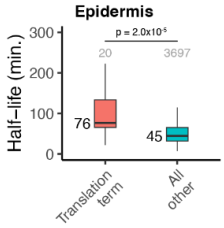

F

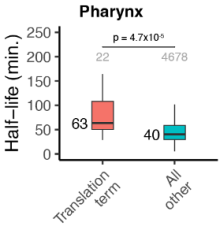

G

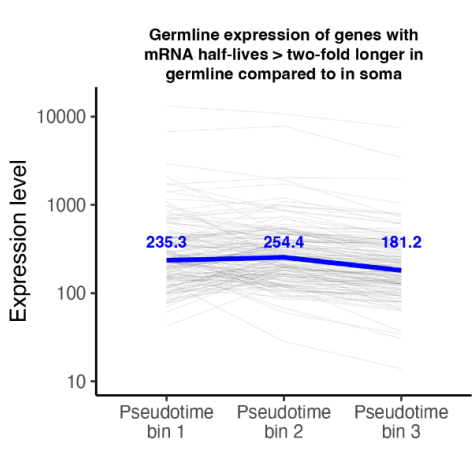

H

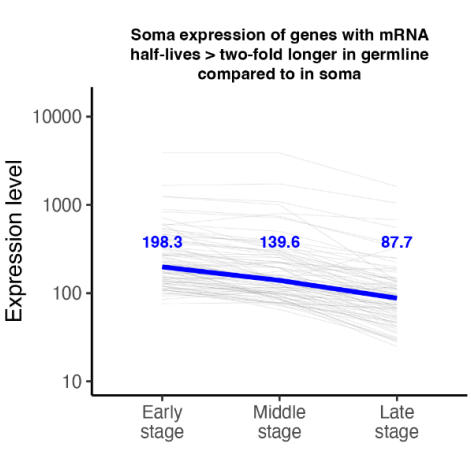

Supplemental Fig S14. Extended analysis of stable transcripts in germline. (A) Gene ontology categories enriched among the top 15% stable transcripts in the germline. Background set of genes used was all germline-expressed genes that met our moderate mRNA half-life filtering metric. (B) Box plots showing the germline-specific mRNA half-life distributions of genes that encode proteins involved in translational elongation and the positive regulation of translation. Numbers to the left of the box plots are median half-lives within each group. Numbers above the box plots are the number of genes within each group. P-value comparing median half-lives was calculated using the Wilcoxon rank sum test. Outliers not shown: from left to right, 0 and 14 genes within each group had mRNA half-lives > 200 minutes. (C) Box plots showing the muscle-specific mRNA half-life distributions of genes that encode proteins involved in translational elongation and the positive regulation of translation. Numbers to the left of the box plots are median half-lives within each group. Numbers above the box plots are the number of genes within each group. P-value comparing median half-lives was calculated using the Wilcoxon rank sum test. Outliers not shown: from left to right, 2 and 92 genes within each group had mRNA half-lives > 200 minutes. (D) Box plots showing the neuron-specific mRNA half-life distributions of genes that encode proteins involved in translational elongation and the positive regulation of translation. Numbers to the left of the box plots are median half-lives within each group. Numbers above the box plots are the number of genes within each group. P-value comparing median half-lives was calculated using the Wilcoxon rank sum test. Outliers not shown: from left to right, 1 and 35 genes within each group had mRNA half-lives > 200 minutes. (E) Box plots showing the epidermis-specific mRNA half-life distributions of genes that encode proteins involved in translational elongation and the positive regulation of translation. Numbers to the left of the box plots are median half-lives within each group. Numbers above the box plots are the number of genes within each group. P-value comparing median half-lives was calculated using the Wilcoxon rank sum test. Outliers not shown: from left to right, 3 and 80 genes within each group had mRNA half-lives > 200 minutes. (F) Box plots showing the pharynx-specific mRNA half-life distributions of genes that encode proteins involved in translational elongation and the positive regulation of translation. Numbers to the left of the box plots are median half-lives within each group. Numbers above the box plots are the number of genes within each group. P-value comparing median half-lives was calculated using the Wilcoxon rank sum test. Outliers not shown: from left to right, 2 and 77 genes within each group had mRNA half-lives > 200 minutes. (G) Germline expression across relative time bins of genes with mRNA half-lives greater than two-fold longer in the germline compared to in the soma. Germline expression in TPM was obtained from a *C. elegans* embryo single-cell atlas (Packer et al. 2019). Blue line is median expression across all genes. (H) Soma expression across Early, Middle, and Late stages of embryogenesis of genes with mRNA half-lives greater than two-fold longer in the germline compared to in the soma. Germline expression in TPM was obtained from a *C. elegans* embryo single-cell atlas (Packer et al. 2019). Blue line is median expression across all genes.